Details of the Electro-Mechanical (E/M) Impedance Health Monitoring of Spot-Welded Structural Joints

Victor Giurgiutiu, Anthony Reynolds, and Craig A. Rogers

Department of Mechanical Engineering, University of South Carolina
Columbia, SC, 29212, USA, 803-777-8018, victorg@sc.edu

ABSTRACT

Health monitoring of structural joints is a major concern of the engineering community. Among joining techniques, spot-welding play a major role. Spot welding is the traditional method of assembly for steel-based automotive structures, while spot-welding of aluminum is being considered for future vehicular structures. Though spot welding of steel is well researched and understood, the spot-welding of aluminum still poses a considerable challenge. The durability and health monitoring of aluminum spot-welded joint is of major importance.

The present paper addresses the use of electro-mechanical (E/M) method and piezoelectric active sensors for health monitoring spot-welded structural joints. Experiments were performed on aluminum-alloy spot-welded lap shear specimens under fatigue loading to determine a stable pattern of crack propagation in correlation with applied fatigue cycles. The specimen stiffness method was used to correlate crack advancement through the specimen with specimen stiffness reduction. In this way, an independent method of assessing the degree of structural deterioration as a function of applied fatigue cycles and remaining life was established for that class of specimens. Then, representative test specimens were instrumented with piezo-electric wafer transducers, and the base E/M impedance signature was recorded over the relevant frequency range. Subsequently, the specimens were subjected to fatigue loading such that crack-type damage was initiated and propagated under controlled conditions. During tests, the specimens were continuously monitored for stiffness reduction, and E/M impedance signature was recorded at predetermined damage levels. The crack damage initiation and propagation was correlated with E/M impedance measurements. Damage index values were compared and correlated with the crack damage propagation. Sources of experimental errors were identified and discussed.

Key Words: Damage detection; Health monitoring; Failure prevention; Electro-mechanical impedance; NDE; Non-destructive evaluation; Incipient damage; Piezo-electric transducer; Crack propagation; Crack detection.

1. INTRODUCTION

Health monitoring of structural joints is a major concern of the engineering community. Among joining techniques, the spot welding and weldbonding (spot weld + adhesive bonding) are widely used in a number of industries. Spot welding is the traditional method of assembly for steel-based automotive structures, while weldbonding is a novel technique that combines the stiffness and productivity benefits of adhesive bonding with the proven-technology attributes of spot welding. Future trends in the design and construction of vehicular structures indicate a strong diversification of material usage, with aluminum and polymeric composites projected to play a major role. While aluminum is amenable to both spot welding and adhesive bonding, composites will, most likely, be entirely adhesive bonded. The trend towards adhesive bonding and weldbonding replacing traditional joining methods is clearly perceived.

In a previous paper, Giurgiutiu *et al.* (1997) performed a review of current NDE methods applicable to spot welded and weldbonded joints. However, none of them were found to be well suited for the present-day requirements for in-situ health monitoring and on-line failure prevention. In the same paper, concepts for adaptive structural health monitoring of this type of joints were developed. In the present paper, experimental results obtained on lap shear specimens of spot-welded joints, using the electro-mechanical (E/M) impedance technique for structural health monitoring, damage detection, and non-destructive evaluation (NDE) will be presented.

2. ELECTRO-MECHANICAL IMPEDANCE

The electro-mechanical impedance method for structural health monitoring, damage detection and NDE was explained in detail by Rogers and Giurgiutiu (1997) and by Giurgiutiu and Rogers (1997). A overview of its principles is given next. Consider a piezo-electric transducer wafer intimately bonded to the surface of a structural member. When excited by an alternating electric voltage, the piezo-electric transducer applies a local strain parallel to the surface. Thus, elastic waves are transmitted into the structure. The structure responds by presenting to the transducer the drive-point mechanical impedance $Z_{str}(\omega) = i\omega m_e(\omega) + c_e(\omega) - ik_e(\omega)/\omega$. Through the mechanical coupling between the PZT transducer and the host structure, and through the electro-mechanical transduction inside the PZT transducer, the drive-point structural impedance directly reflects into the effective electrical impedance as seen at the transducer terminals (Figure 1).

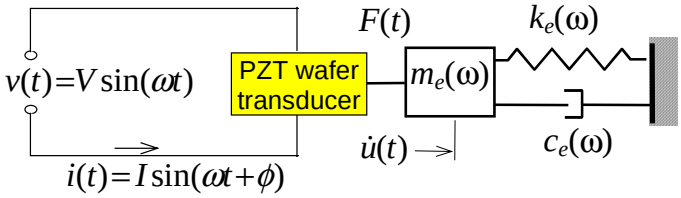

Figure 1 Electro-mechanical coupling between the PZT transducer and the structure.

The electro-mechanical (E/M) impedance technique for health monitoring, damage detection, and NDE (Rogers and Giurgiutiu, 1997) utilizes the changes that take place in the drive-point structural impedance to identify incipient damage in the structure. The apparent electro-mechanical impedance of the piezo-transducer as coupled to the host structure is given by

$$Z(\omega) = \left[i\omega C \left(1 - \kappa_{31}^2 \frac{Z_{str}(\omega)}{Z_{PZT}(\omega) + Z_{str}(\omega)} \right) \right]^{-1}. \qquad (1.)$$

In Equation (1), $Z(\omega)$ is the equivalent electro-mechanical admittance as seen at the PZT transducer terminals, C is the zero-load capacitance of the PZT transducer, and κ_{31} is the electro-mechanical cross coupling coefficient of the PZT transducer ($\kappa_{31} = d_{13}/\sqrt{\bar{s}_{11}\bar{\varepsilon}_{33}}$). The mechanical impedance of the structure is Z_{str}, while that of the PZT transducer is Z_{PZT}. As seen in equation (1), the interaction of the structural and transducer mechanical impedance modifies the effective electrical impedance as measured at the transducer terminals. This frequency dependent process is highly coupled with the internal state of the structure, as reflected in the drive-point mechanical impedance, Z_{str}. The electro-mechanical impedance method is applied by scanning a predetermined frequency range in the hundreds of kHz band and recording the complex impedance spectrum. By comparing the impedance spectra taken at various times during the service life of a structure, meaningful information can be extracted pertinent to structural degradation and the appearance of incipient damage. It must be noted that the frequency range must be high enough for the signal wavelength to be compatible with the defect size.

3. SPOT-WELDED LAP-JOINT SHEAR SPECIMEN

3.1 Description of the Specimen

A spot welded lap-joint shear specimen was used in this experiment. Figure 2 presents a spot-welded lap-joint specimen instrumented with 12 PZT wafer transducers. The numbers represent the transducer stations arranged in flip-side pairs on the specimen. The lap joint was constructed from dissimilar alloys, aluminum 7075-T6 and 2024-T3. This particular combination of materials chosen presents interest for the production of built-up skin-stringer structures with aerospace applications. Nominal thickness of the specimen was 2-mm (80-mil). Specimen width was 25.4-mm (1-in) and length 167-mm (6.5-in). The overlap length was 36 mm (1.5-in). Spot weld size was 9-mm (0.354-in).

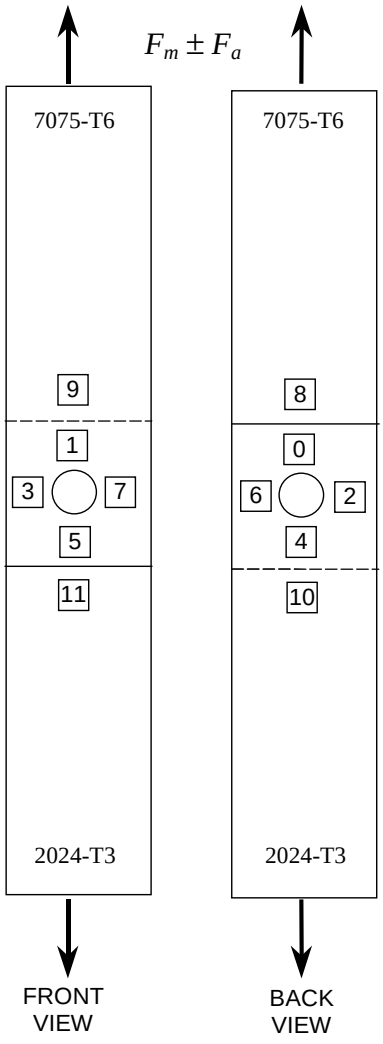

Figure 2 Spot-welded lap-joint specimen schematic.

3.2 Instrumentation of the Specimen

The specimen was instrumented with 12 square-shaped piezo-electric wafer transducers of 6-mm (1/4-in) size (Figure 2). The wafer transducers were manufactured in the Laboratory for Adaptive Material Systems and Structures (LAMSS), Department of Mechanical Engineering, University of South Carolina. Piezoelectric transducer were fabricated from PZT (Lead Zirconate Titanate) single sheets supplied by Piezo Systems, Inc., Part # T107-H4ENH-602. The as-supplied PZT sheets were of dimensions 2.85-in × 2.85-in (72-mm × 72-mm) in had a thickness of 190-μm (7.5-mil). The sheets were cut into 6-mm strips, and then into small (6 mm × 6 mm) PZT squares using proprietary methods. The small PZT squares were affixed onto 25-μm (1-mil) copper foil using specialized bonding methods. The assembled transducer was mounted onto the specimen using Micro Measurements, Inc. strain-gauge-mounting technology.

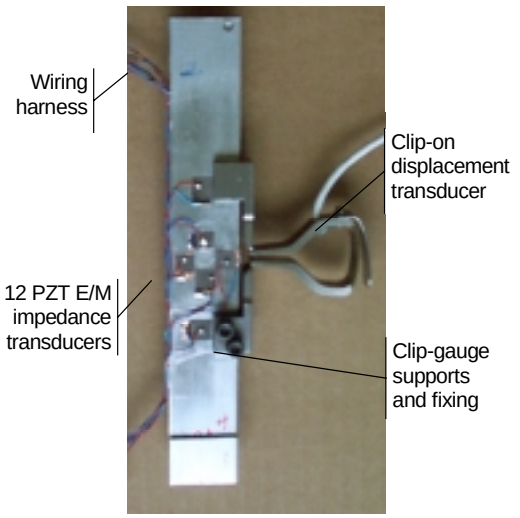

Figure 3 Photograph of the spot-welded lap-joint specimen instrumented with bonded PZT transducers and a clip-on displacement transducer.

The transducers were wired and numbered. Through the process, the electrical integrity of the transducers was measured for consistency. Rejects were dismounted and re-instrumented. Finally, support fixtures and the clip-on displacement transducer manufactured by John A. Shepic, Lakewood, Colorado, were attached. The instrumented specimen is presented in Figure 3. Using an Hewlett Packard 4194A Impedance Analyzer, the E/M impedance signatures of the 12 PZT transducers affixed to the specimen was taken and stored in the PC as baseline information. The frequency range 200 to 1100 kHz was determined as best suited for this process.

4. EXPERIMENTAL PROCEDURE

4.1 Loading Conditions

The spot-welded lap-joint specimen was mounted into an MTS 810 Material Test System, as shown in Figure 4. Tension-tension fatigue testing at R = 0.1 and a max load of 2.67-kN was performed. The load path in the lap-joint specimen is eccentric and produces a combined tension-bending load condition. The typical ultimate load for the spot weld specimens is approximately 8-kN. Under this set of fatigue loading, the specimen fatigue life does not exceed 45,000 cycles.

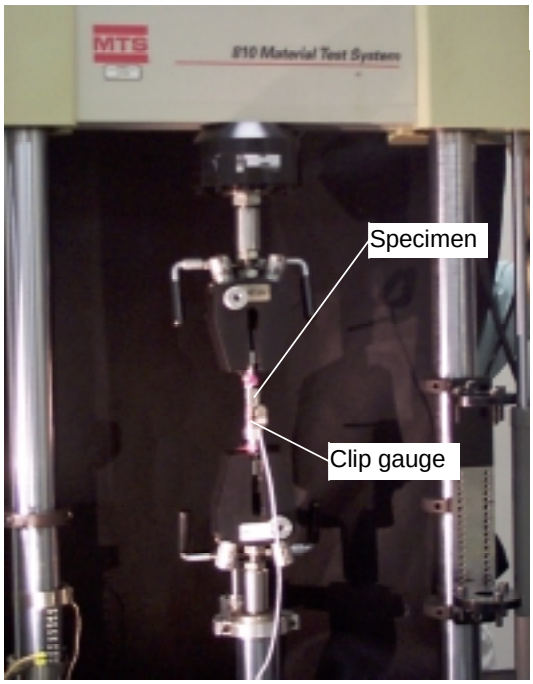

Figure 4 Spot-welded lap-joint specimen mounted in the MTS 810 Material Test System for fatigue crack propagation studies.

4.2 Generation of Controlled Damage

Generation of controlled damage in experimental specimens is a major concern for any health monitoring and damage detection experiment. In the present study, our primary goal was to correlate changing E/M impedance signals with varying levels of fatigue damage in the spot welded joint. Hence, a repeatable method of identifying and quantifying specimen damage at any point in time was devised.

4.2.1 Nature of Damage

In the spot-welded lap-joint specimen, fatigue cracks develop as follows: A surface crack initiates at the weld nugget/base metal interface in the 7075-T6 half of the weld specimen. Then, the surface crack grows around the periphery of the weld nugget while at the same time penetrates through the sheet thickness. After the crack penetrates the sheet, it extends in the same manner as a through crack in a center-cracked plate. At the load levels used in this study, the great majority of fatigue life is consumed before the crack penetrates the sheet thickness.

In some cases, overload fracture might occur before the crack penetrates the sheet thickness. Figure 5 is a visible light optical fractograph showing the general shape of the fatigue crack in one half of a fractured overlap shear spot weld specimen. The initiation site is on the original faying surface of the welded specimen and the black line separates the fatigue failure from the overload fracture.

4.2.2 Damage Quantification

Damage quantification and control was performed using stiffness-damage correlation principle. It has long been known that a direct correspondence exists between stiffness loss in a fatigue specimen and damage progression under repetitive (fatigue) loading. Razvan, Reifsnider, and Elahi (1994) have shown that a direct relationship can be established between stiffness reduction and damage progression in materials under cyclic loading. Hence, dynamic characterization can be implemented during fatigue testing to estimate the extent of crack progression and the remaining life of the structure. Although spot weld fatigue tests are typically used to develop S-N data, it was surmised that fatigue damage could be monitored by observing changes in specimen stiffness as a function of number of fatigue cycles. Previous studies have shown stiffness changes in spot-welded structure; however, these studies typically used machine ram displacement rather than actual specimen displacement resulting in some anomalous and misleading stiffness vs. life correlation (Salvini et al., 1997). In our experiments, we generated controlled damage through fatigue loading and stiffness monitoring. Real time monitoring of specimen stiffness was done using the load signal from the MTS force gauge and the displacement signal from the clip-on gauge placed across the spot weld (Figure 3). The load signal and the displacement signal are processed using a fatigue crack growth test control and data acquisition program originally designed to monitor specimen compliance for determination of crack length in da/dN-ΔK testing. The result is a nearly continuous record of specimen stiffness as a function of fatigue life. While both spot weld fatigue life and initial spot weld stiffness exhibit significant scatter, previous testing (Chassereau and Reynolds, 1998) has shown that a simple normalization procedure can be used to collapse all the data from tests performed under a single set of conditions. By dividing the instantaneous values of stiffness loss and fatigue cycles, normalized by the initial stiffness and by the fatigue cycles to failure, respectively, we generated "% stiffness loss" and "% cycles to failure". After normalization, the results from several fatigue tests fell into a narrow scatterband (Figure 6).

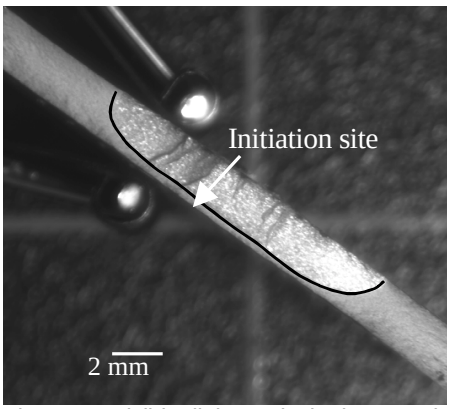

Figure 5 Visible light optical photograph of the fatigue fracture in a spot weld. The black line outlines the region of fatigue failure.

This forms the basis of the stiffness-damage correlation principle indicating that a one-to-one correspondence can be established between stiffness loss in the specimen and accumulated cycles to failure (i.e., damage). Thus, by monitoring stiffness loss, we could actually monitor and control the amount of damage accumulating in the fatigue specimen.

4.3 Health Monitoring under Controlled Damage Conditions

The stiffness-damage correlation principle was used to identify and control the damage progression in the spot-welded lap-joint shear specimen during the fatigue testing. Our purpose was to stop the loading and collect health-monitoring data at predetermined damage (stiffness loss) values. This was achieved by monitoring the stiffness during fatigue cycling, and stopping the experiment when the it dropped to 95%, 90%, 80%, 70%, 65%, 60%, 55% of the initial stiffness value. These data points correspond to 5%, 10%, 20%, 30%, 35%, 40%, and 45% stiffness loss.

At each stiffness value, readings were taken of the E/M impedance signature of the 12 PZT transducers and stored in the PC.

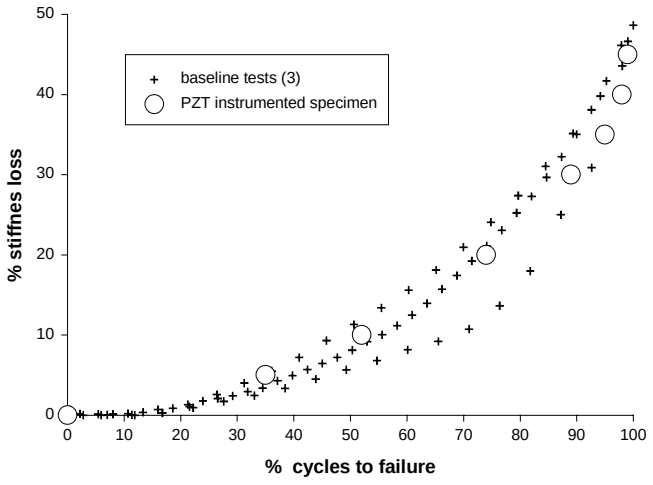

Figure 6 Graph of percentage stiffness loss vs. percentage cycles to failure for lap-shear spot weld specimens tested at P_{max} = 2.7-kN and R=0.1

The process was repeated until the specimen broke (32,260 cycles, 54% of initial stiffness, Figure 7). To verify our assumptions, the data points obtained in this experiment were superposed (plotted as circles) on the stiffness-life correlation curve of Figure 6 that already contained results from three previously performed fatigue tests on similar specimens under similar loading (plotted as crosses). As shown, the current experiment fits very well into the rest of the data, indicating that the stiffness-damage correlation principle can be used to this study.

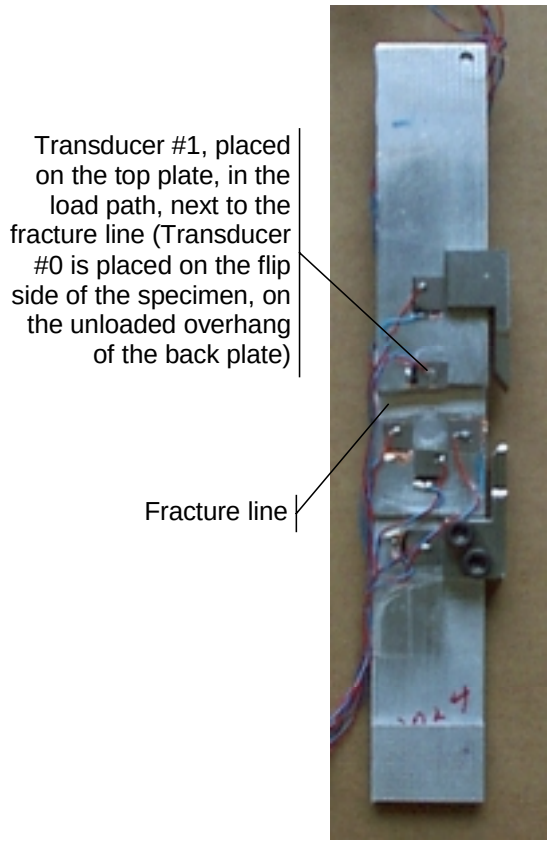

Figure 7 Post-failure presentation of the spot-welded lap-joint shear specimen. Failure occurred after N = 32,260 cycles, at 54% stiffness.

5. RESULTS

Figure 8 presents, for each of the twelve E/M transducers, superposed plots of the impedance signatures obtained at various levels of stiffness loss. The impedance signatures considered here are the real part of the complex E/M impedance, Z, measured in the frequency band 200 – 1,100 kHz. (The frequency band was selected during pre-trial tests). Examination of the 12 graphs contained in Figure 8 reveals important modifications taking place in the impedance signatures due to intricate structural response changes induced by damage progression. However, direct interpretation of these impedance signatures is not straightforward. A more direct interpretation could be attained through the use of a *damage index*. The damage index is a scalar quantity that is evaluated from the comparison of impedance signature at a given damage level with a baseline signature. In our experiment, we took as baseline the signature of the pristine specimen. The mathematical expression of the damage index can be varied, and depends on the choice of damage metric. In this work, we used a damage index based on the Euclidean norm, i.e., the RMS impedance change calculated as:

$$\text{RMS Impedance Change, \%} = \left(\frac{\sum_{N} \left(\text{Re}\, Z_i - \text{Re}\, Z_i^0 \right)^2}{\sum_{N} \left[\text{Re}(Z_i^0) \right]^2} \right)^{1/2} \qquad (2.)$$

In Equation (2), N is the number of sample points in the impedance signature spectrum, while the superscript 0 signifies the initial (baseline) state of the structure.

6. DISCUSSION

6.1 Description of Damage

In this spot welded specimen, the damage is highly localized. Damage appears in the form of a progressive crack, initiated at the spot weld boundary and propagating across the width and thickness of the specimen. A typical crack geometry was shown in Figure 5. The crack propagates simultaneously, on a arced front, in the thickness and width directions, until it penetrates across the plate thickness. Subsequently, the propagation takes place sideways, in the typical manner of a through-the-thickness crack propagation. As the crack advances, the effective stiffness of the specimen decreases. Changes are also induced in the effective boundary conditions for local plate vibrations. The crack propagation induces specific changes in the local high-frequency response. The point-wise mechanical impedance presented to the E/M transducers is also modified. This reflects in changes in the E/m impedance spectrum.

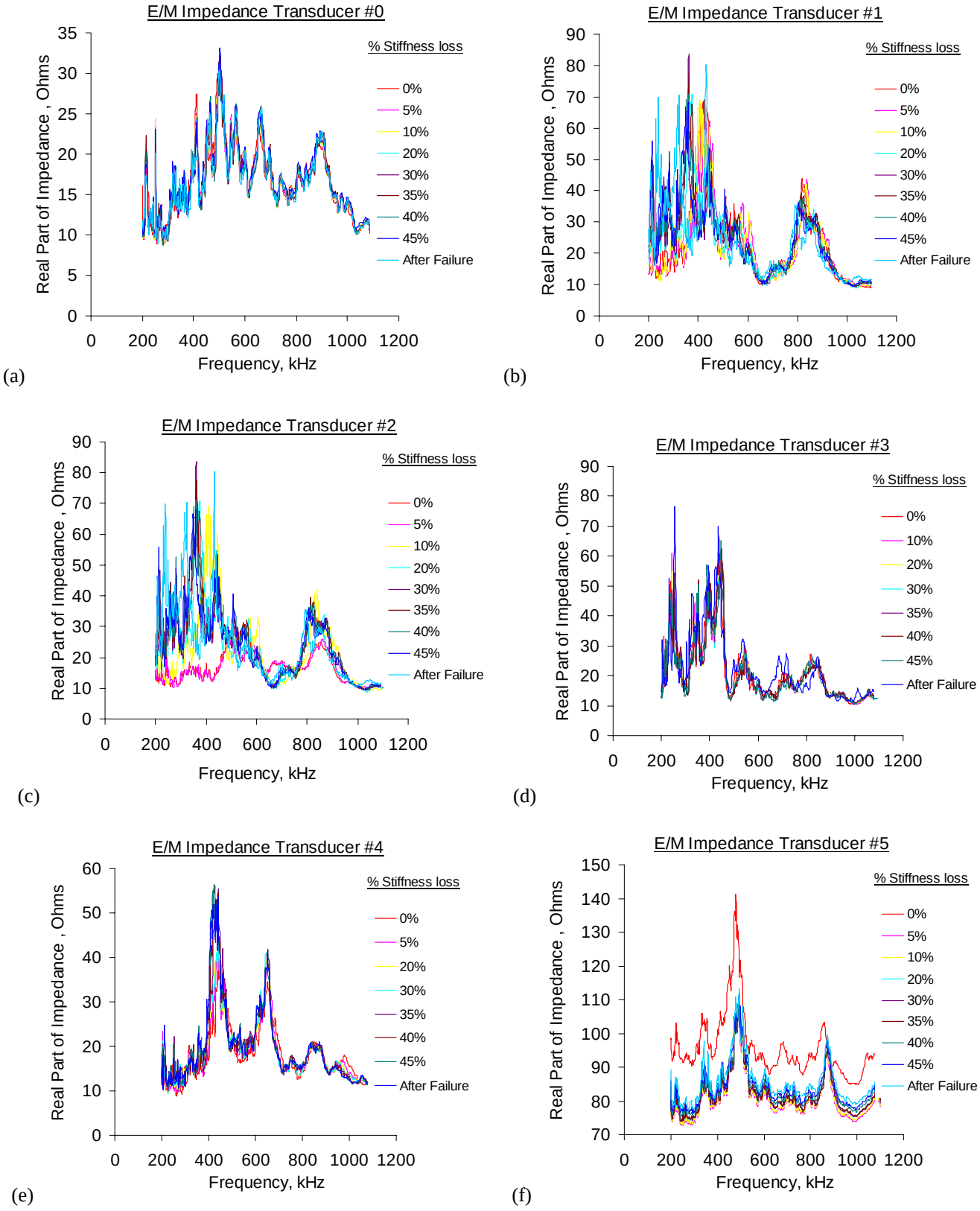

Figure 8 Superposed plots of impedance signatures of E/M transducers for increasing amounts of specimen stiffness loss, transducers #0 through 5 (also available for viewing in color at http://www.engr.sc.edu/research/lamss/spot1a.htm)

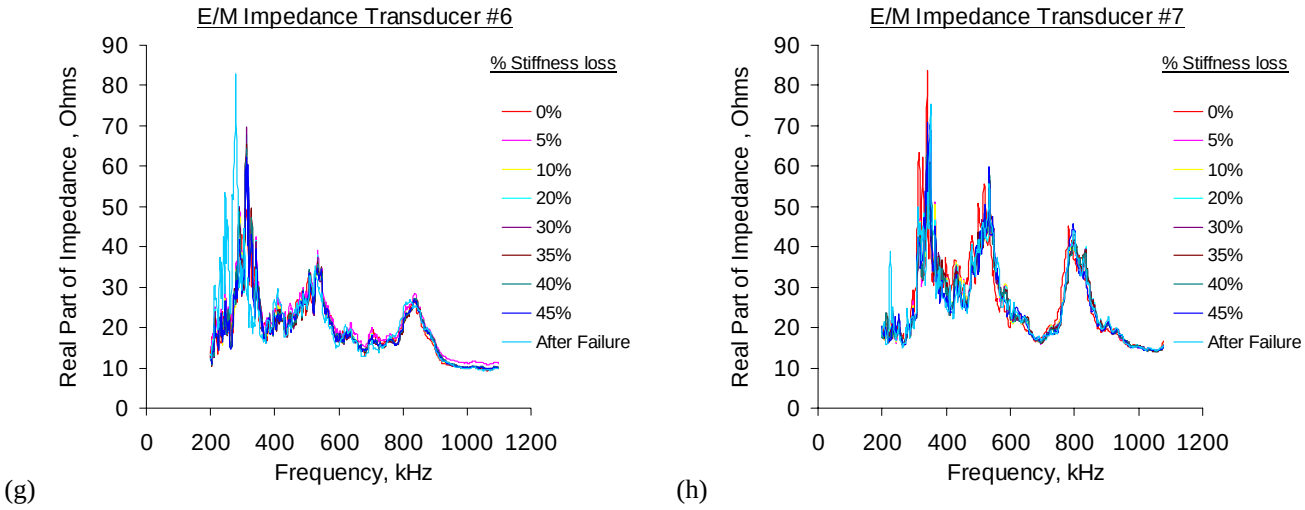

(g)

(h)

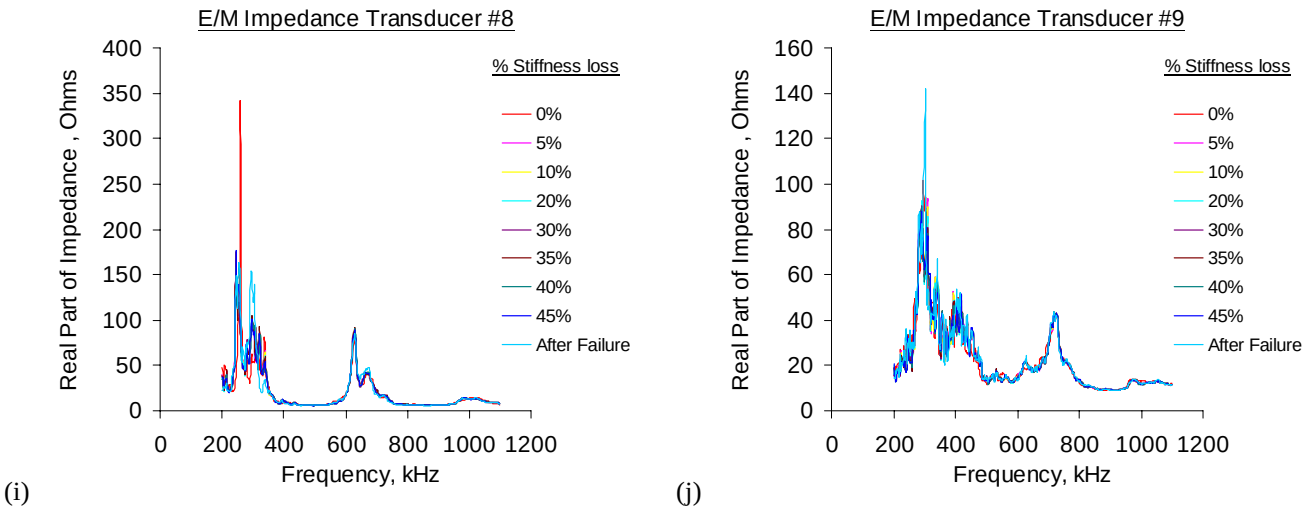

(i)

(j)

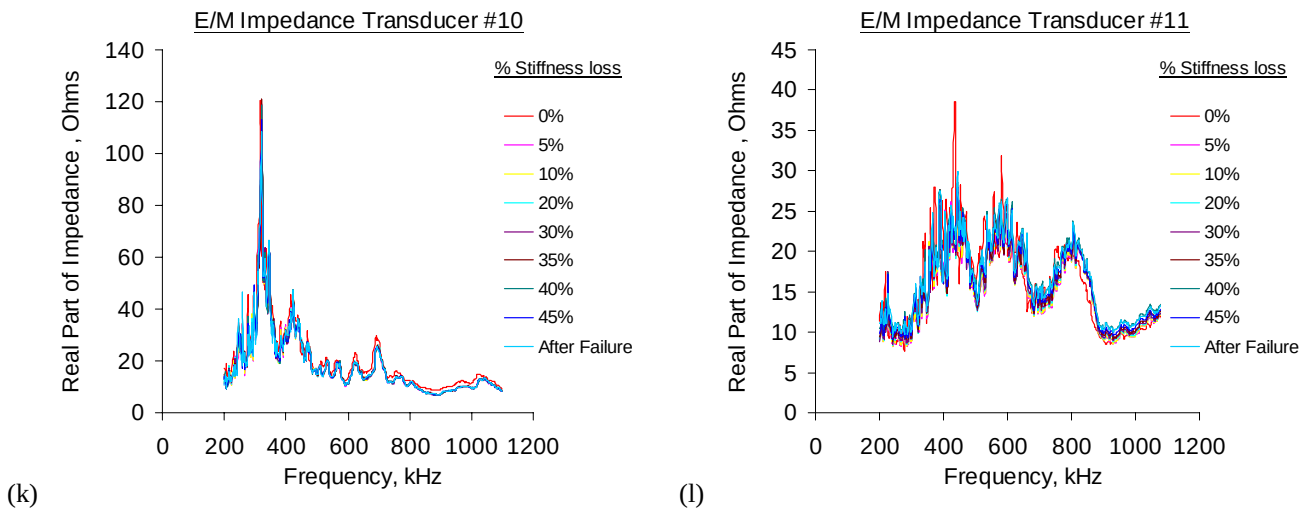

(k)

(l)

Figure 8 (cont.) Superposed plots of impedance signatures of E/M transducers for increasing amounts of specimen stiffness loss, transducers #6 through 11 (also available for viewing in color at http://www.engr.sc.edu/research/lamss/spot1a.htm)

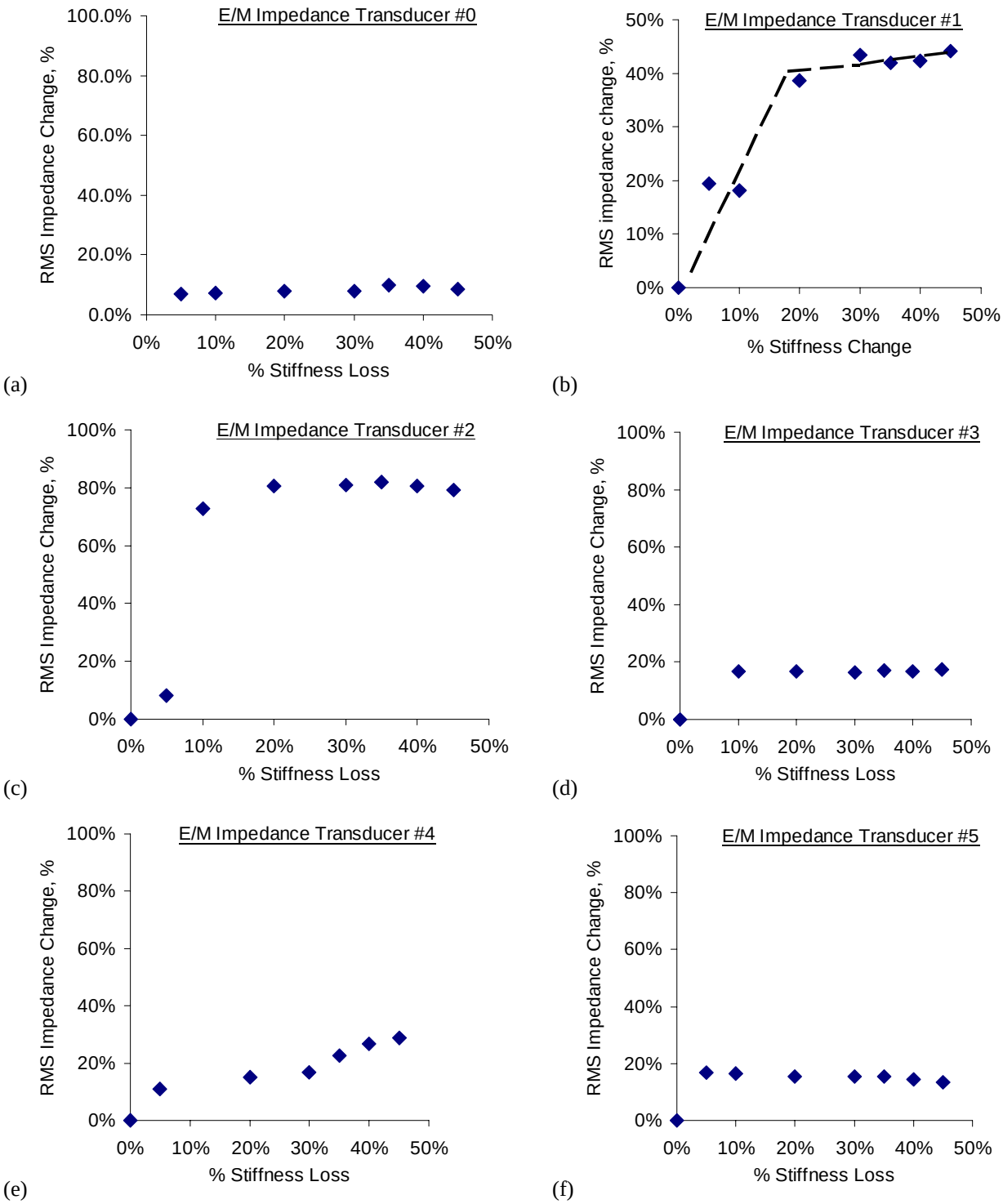

Figure 9 Correlation between RMS impedance change and specimen stiffness loss, as recorded by each transducer (transducers #0 through 5)

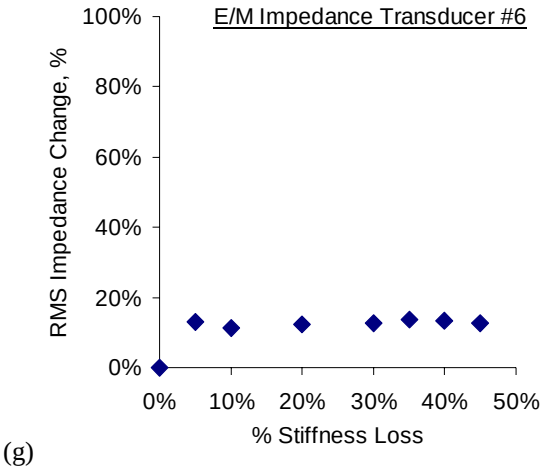

(g)

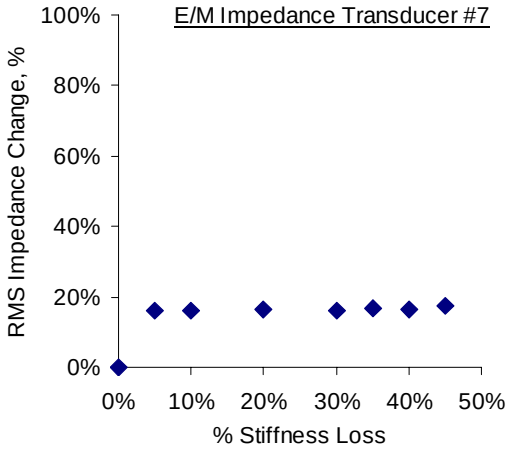

(h)

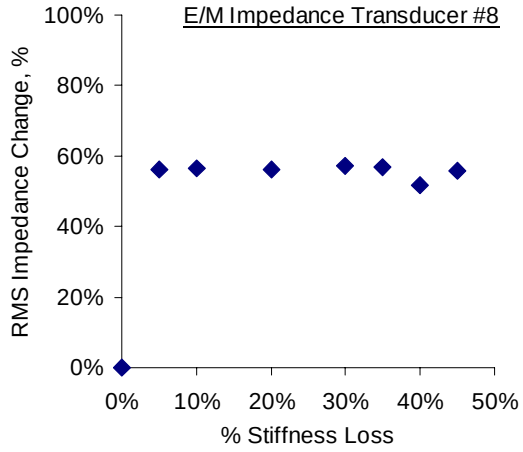

(i)

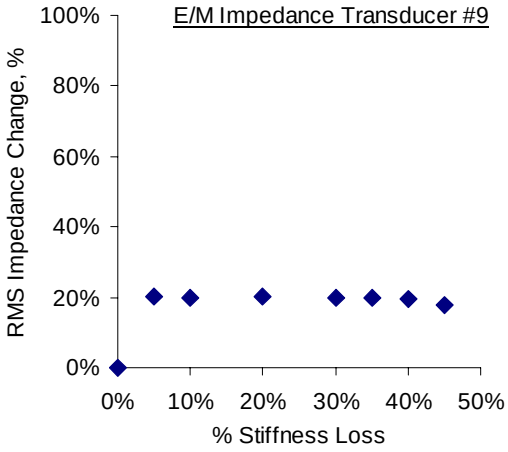

(j)

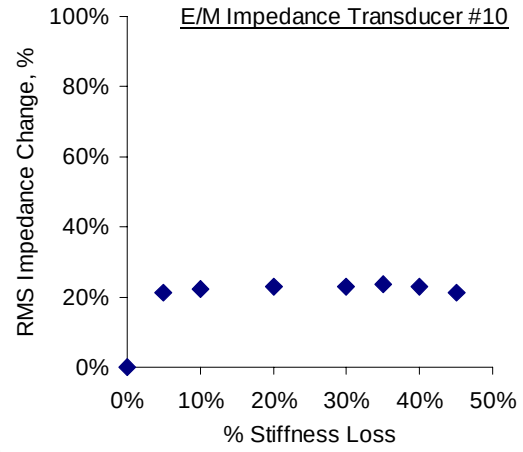

(k)

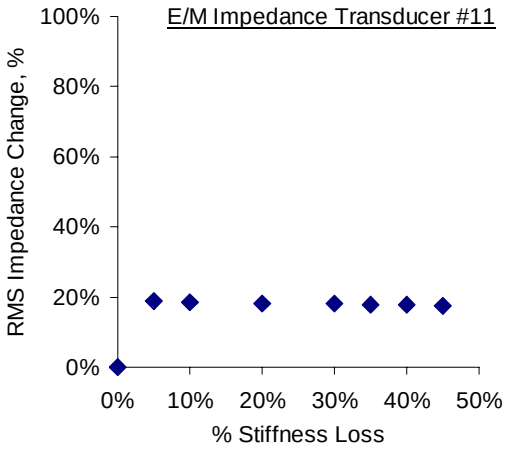

(l)

Figure 9 (cont.) Correlation between RMS impedance change and specimen stiffness loss, as recorded by each transducer (transducers #6 through 11).

6.2 Correlation of E/M impedance readings with stiffness reduction and damage progression.

Examination of the E/M impedance data reveals changes recorded in the E/M impedance signatures with the progression of damage. These changes are reflected in both the E/M impedance signatures (Figure 8) and in the RMS impedance change curves (Figure 9). Due to the good localization properties of the E/M transducers, only the transducer placed in the area of influence of the damage are expected to be sensitive to the presence of damage and its progression. For our specimen, this is the case with transducer #1. The rest of the E/M transducers, were placed farther away from the damage area, did not respond directly to damage progression. The following sections treat these two situations in details.

6.2.1 Behavior of E/M Transducer #1

Figure 8b presents the superposed plots of impedance signatures of transducer #1 for increasing amounts of structural damage. Examination of Figure 8b indicates that significant changes took place in the E/M impedance signature as damage progressed through the specimen. New frequency peaks appeared at approximately 250 and 300 kHz, while the peak at 400 kHz was greatly accentuated. Figure 9b gives a plot of the RMS impedance change versus percentage stiffness loss. The RMS impedance change curve for E/M transducer #1 presents three distinct regions: A linear slope region, in which the damage-index values increase monotonically with the stiffness loss. This region corresponds to the crack propagating in the proximity of transducer #1. Because of the proximity between crack and transducer, the changes due to the crack are directly sensed by the E/M transducer.

(i) The plateau region in which the RMS impedance change is stationary. This region corresponds to the crack boundaries propagating far away from the E/M transducer. Once the crack boundary has extended away from the transducer, consequent crack growth no longer affects the transducer readings.

(ii) A final-break region, in which the damage-index increases higher than the plateau value. This jump corresponds to changes taking place as final breakage of the structure occurs.

These observations show that the RMS impedance change, calculated with formula (2), is a valid quantitative indicator of the amount of structural damage adjacent to the transducer. The quantitative information given by the RMS impedance change can be usefully leveraged into life prediction studies.

6.2.2 Behavior of the other E/M transducers

The other E/M transducers besides transducer #1 were not influenced by the crack propagation, since they were away from crack boundaries. (Transducers #3 and #7 were somehow closer to the crack boundary, but placed in the proximity of the spot weld. Since the spot weld did not fail and remained intact during the tests, these two transducers were shielded from the influence of the crack by the much stiffer influence of the weld.) Overall, the following comments can be made regarding the behavior of the E/M transducers that outside the influenced of crack damage propagation in the specimen:

Transducers #0, #3, #4, #5, #6, #7, #9, #10, and #11 showed a sudden RMS impedance change at the first reading after loading (e.g., Figure 9a). The amplitude of this sudden change is small (10-20%). Subsequently, the value of the RMS impedance change remained more or less constant while damage progressed. We attribute this RMS impedance change to readjustment of the E/M gauges after the initial loading of the specimen. This is an artifact, and is not connected with actual damage progression. In practical implementation of the method, moving the baseline reading from the unloaded condition to the condition after first loading cycle could compensate this artifact.

Transducers #2 and #8 show similar plateaus in the RMS impedance change behavior, but of larger amplitudes (80% for transducer #2 and 60% for transducer #8). Again, this behavior is explainable through changes induced by the initial loading of the specimen. Careful examination the E/M impedance signatures for transducers #2 and #8 (Figure 8c and i) indicates dramatic changes in the signature pattern happening at the beginning of the loading cycles. For transducer #2, the E/M impedance signatures at zero damage, and after the initial loading block, show much lower activity than the other signatures. For transducer #8, the initial signature has a strong resonance spike, which subsequently does no longer appear. Examination of transducer #8 under visual magnification reveals that it has become partially disbonded from the specimen. Hence, its indications are considered flawed and have to be discarded. We believe that a similar change also happened to transducer #2, though it is not readily detectable with visual means.

6.3 Sensitivity, Localization, and Rejection Properties of the E/M Impedance Method

Sensitivity, localization, and rejection are important properties of any health monitoring method. Sensitivity indicates that the

transducers respond well to the presence of damage. Good transducer sensitivity is essential for the method success. Localization means that the transducers response in limited to a localized area of the structure. Good localization ensures that position of the damage can be easily identified using a transducer array. Rejection refers to the transducer not being influenced by spurious signals, or by the normal operation of the monitored structure or machinery. The data presented in the previous sections proved the sensitivity, localization, and rejection properties of the E/M impedance method. Transducer #1, placed in the crack vicinity, responded very well, while the rest of the transducers, placed outside the crack area of influence, did not show significant response. Thus, sensitivity and localization are verified. Rejection is also satisfied since the E/M impedance method operates at very high frequency (200 – 1,100 kHz), which is well above the bandwidth of normal machinery vibrations.

6.4 Elementary Explanation of the Damaged Spot-Welded Lap-Shear Specimen Behavior

Figure 10a shows a side view of the spot-welded lap-shear specimen. The top and bottom plates are joined by the spot weld. Careful examination of the joint area reveals the top and bottom plates do not actually touch. Between the two plates, a gap of approximately 0.300-mm exists. The top and bottom plates can be considered to vibrate without interference between them, their only connection being through the spot weld. Due to symmetry, the spot weld presents built-in-support boundary conditions for the symmetric modes, and pin support boundary conditions for the anti-symmetric modes.

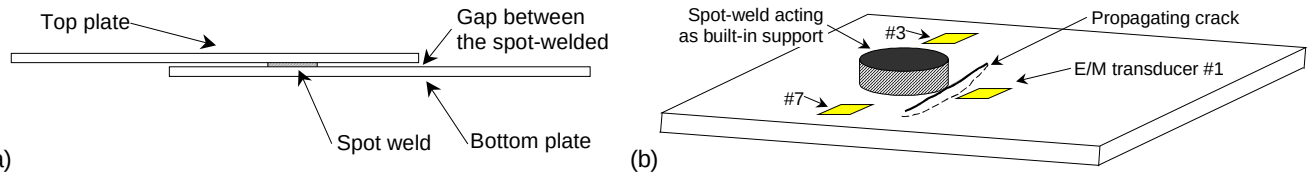

Figure 10 Details of the spot-welded lap-shear tension specimen: (a) Side view of a spot-welded lap-shear specimen featuring the top and bottom plates, the spot weld, and the gap between the plates. (b) Representation of the bottom plate of the spot-welded lap-shear specimen with a crack propagation close to the spot weld. The plate boundary conditions are radically changed as the crack propagates.

As a crack forms and advances in the plate next to the spot weld, the boundary conditions change (Figure 10b). The area of influence of the boundary conditions depends on the vibration wavelength. Our tests were conducted at high frequency in the range 200 to 1,100 kHz. For a median frequency of, say, 500 kHz, the typical flexural wavelength has the value around 5-mm. Thus, the area of influence of the boundary conditions is restricted to the spot weld and crack vicinity. The only transducer present in the area of influence was transducer #1. This transducer was shown sensitive to the crack presence, as shown in Figure 8b. The rest of the transducers were outside the area of influence of the crack, and did not show a distinct response. Please also note that the RMS impedance change response of transducer #1 flattens out after reaching the 40% mark in Figure 9b. The explanation for this phenomenon lies in the fact that, beyond the 40% damage mark, the crack has propagated beyond the transducer proximity, and hence its influence is no longer detectable. This explanation confirms the good localization properties of the E/M transducers.

7. CONCLUSIONS

An important application of the E/M impedance method to the health monitoring, damage detection, and NDE of spot-welded structural joints has been presented. To authors knowledge, this is the first time that the E/M impedance method has been applied to the NDE of this type of joints. Incremental damage tests of spot-welded lap-joint shear specimens under fatigue loading were performed. The stiffness-damage correlation principle was used to quantify progression of damage. The experimental data collected during these tests showed that the E/M impedance signature, and the resulting damage index, could be directly correlated with the structural damage progression. Through the used of multi-site E/M impedance measurements, the sensitivity, localization, and rejection, properties of the method have also been verified. The data presented in this paper indicates that:

1) Specimen stiffness may be used as a measure of spot-weld fatigue damage.
2) Reproducible amounts of fatigue damage can be introduced in the specimen. Thus, NDE techniques can be calibrated.
3) The E/M impedance data correlates with the damage level in the spot weld.

4) Changes in E/M impedance signatures from individual PZT transducers depend on transducer position relative to the damage site. Thus, a transducer array can be devises to provide information on both the level and the location of damage.
5) The correspondence between remaining life and stiffness loss observed for several different loading levels in spot-welded specimen (Chassereau and Reynolds, 1998) can be extended to any repetitive fatigue-loading spectrum. Thus, the E/M impedance method can be calibrated to indicate the remaining life of the structure for a given loading spectrum.

Improvements of the E/M impedance technique are needed especially in the area of transducer fabrication and attachment. This work is currently under way in the Department of Mechanical Engineering at the University of South Carolina.

The work presented in this paper indicates that the E/M impedance data may be successfully used for health monitoring and remaining fatigue life estimation of spot-welded structural joints. In-situ arrays of E/M transducers placed on aging structures are envisioned. Through local-area data collection, interpretation, wide-area tele-transmission, and automatic system for health monitoring and damage detection can be devised and installed. The use of a damage index will allow rapid estimation of the structural health condition in terms of a single scalar value. This will open the path for computer-controlled data interpretation and damage assessment. Existing aging structures and future new structures can be equally considered as potential applications. Important safety enhancement and significant cost savings are predicted through the wide area implementation of this novel method for structural health monitoring, damage detection, and failure prevention.

Significant work needs still to be done to ensure consistency, reliability, and market acceptability of this new method. Directions for further work include standardization of sensor fabrication and attachment, perfection of damage index calculation, miniaturization of impedance measuring apparatus, and development of a data-gathering network. Such work is currently under way, and will be the presented in the near future.

ACKNOWLEDGMENTS

The authors gratefully acknowledge the financial support of the National Science Foundation through NSF/EPSCoR Cooperative Agreement No. EPS-9630167. The authors would also like to express thanks to Florin Jichi, Graduate Research Assistant, and to Shannon Whitley, Undergraduate Summer Research Intern, for their contribution to data collection and data processing.

REFERENCES

1. Chassereau, L., and Reynolds, A. 1998, “Monitoring and Characterization of Damage Progression in Spot Welds” (in preparation).
2. Giurgiutiu, V., and Rogers, C. A., 1997. "The electro-mechanical (E/M) impedance method for structural health monitoring and non-destructive evaluation", International Workshop on Structural Health Monitoring, Stanford University, CA, September 18-20, 1997.
3. Giurgiutiu, V., Rogers, C. A., Chao, Y. J., Sutton, M. A., and Deng, X., "Adaptive Health Monitoring Concepts for Spot-Welded and Weld-bonded Structural Joints", Proceedings of the ASME Aerospace Division, AD-Vol. 54, ASME, November 1997, pp. 99-104.
4. Razvan, A., Reifsnider, K. L., Elahi, M., 1994, "Dynamic Characterization of Material Strength and Life under Cyclic Loading.” Patent No. 5,305, 645, April 26, 1994, Durability, Inc., Blacksburg, VA.
5. Rogers, C. A. and Giurgiutiu, V., 1997. “Electro-Mechanical (E/M) Impedance Technique for Structural Health Monitoring and Non-Destructive Evaluation”, Invention Disclosure No. 97162, University of South Carolina Office of Technology Transfer, July 1997.
6. Salvini, P., Scardecchia, E., and Demfonti, G., “A Procedure for Fatigue Life Prediction of Spot Welded Joints”, Fatigue and Fracture of Engineering Materials and Structures, vol. 20, no. 8, pp. 1117-1128, 1997.
7. Liang, C., F. P. Sun, and C. A. Rogers, 1993, "An Impedance Method for Dynamic Analysis of Active Material Systems, Proceedings, 34th AIAA/ASME/ASCE/AHS/ASC SDM Conference, La Jolla, CA, 19-21 April 1993; pp. 3587-3599.
8. Liang, C., F. P. Sun, and C. A. Rogers, 1996. “Electro-mechanical Impedance Modeling of Active Material Systems,” Smart Materials and Structures, Vol. 5, pp. 171-186.